A Weather-Aware Risk Stratification Framework for RLF Prediction Using Contrastive Autoencoders and Survival Analysis

M M Sadman Shafi
Department of Electrical and Electronic Engineering
Islamic University of Technology
Gazipur, Bangladesh
sadmanshafi@iut-dhaka.edu

Tasnia Siddiqua Ahona
Department of Electrical and Electronic Engineering
Islamic University of Technology
Gazipur, Bangladesh
tasniaahona@iut-dhaka.edu

Yasin Hasan Saad
Department of Electrical and Electronic Engineering
Islamic University of Technology
Gazipur, Bangladesh
yasinsaad@iut-dhaka.edu

Abstract*— Ensuring reliable radio connectivity in next-generation wireless networks is critical, particularly under dynamic weather-induced impairments that significantly influence link stability. Traditional Radio Link Failure (RLF) prediction approaches primarily focus on binary classification, failing to estimate when a failure is likely to occur. In this work, we propose a novel weather-aware RLF prediction framework that integrates multi-modal feature fusion, contrastive representation learning and survival analysis to produce interpretable time-to-failure estimates. Using a real-world dataset from Turkcell comprising radio key performance indicators (KPIs) and measurements from weather stations, we first employ a supervised autoencoder to learn a fused latent representation of triplet-based meteorological features. A contrastive autoencoder trained with triplet loss then captures discriminative latent embeddings, stratifying links into high and low reconstruction error groups. Survival analysis, leveraging Kaplan–Meier and Nelson–Aalen estimators, demonstrates that higher reconstruction errors correlate strongly with accelerated failure risk, providing actionable insights into temporal link reliability. Furthermore, we incorporate Isolation Forest anomaly detection on learned representations to enhance predictive capability under imbalanced data conditions. Experimental results show that our proposed methodology achieves robust performance in modeling the temporal dynamics of RLF, enabling proactive resource allocation, optimized handover scheduling, and informed Service Level Agreement (SLA) risk management in weather-sensitive wireless environments.

Keywords*— Radio Link Failure, Contrastive Autoencoder, Survival Analysis, Weather-Aware Networks, Predictive Reliability Modeling

I. INTRODUCTION

A communication network can be broadly defined as a system of interconnected nodes that enables the exchange of information, resources, and services across wired or wireless links. In the context of cellular wireless networks, maintaining reliable connectivity between the user equipment (UE) and the base station is critical to ensuring seamless communication. However, this connectivity can be disrupted by a Radio Link Failure (RLF)**,** which occurs when the quality of the radio link degrades below acceptable thresholds due to factors such as fading, interference, mobility or hardware issues. RLF not only interrupts ongoing data transmission and degrades user experience but also imposes additional signaling overhead on the network, leading to inefficient resource utilization and potential degradation of overall network performance.

In 5G networks, radio link reliability is significantly influenced by weather conditions such as rain, humidity, and temperature variations. These environmental factors introduce attenuation and changes in multipath propagation, often resulting in intermittent yet critical (RLF). A binary prediction of RLF, which only indicates whether a failure will occur, is insufficient for proactive network management. Instead, it is more valuable to estimate when a link is likely to fail. This motivates the use of survival analysis, where link degradation is modeled as a time-to-event problem. Techniques such as the Kaplan–Meier estimator enable the construction of survival curves without strong distributional assumptions, while hazard functions capture the instantaneous risk of failure at different points in time. Together, these tools provide a more informative and actionable framework for understanding and predicting the timing of RLF under weather-driven impairments.

At the same time, modern representation learning techniques such as contrastive and latent-clustering encoders can generate compact and noise-resilient feature embeddings. These embeddings capture underlying patterns and subpopulation structures in the data, which in turn enhance the accuracy of time-to-event prediction under censoring.

Building on these ideas, this paper combines a contrastive autoencoder trained on multi-modal inputs (radio telemetry and local meteorological data) with survival analysis methods. Specifically, Kaplan–Meier survival curves and hazard curves are used to generate per-link, calibrated time-to-failure predictions that are both interpretable and actionable, supporting tasks such as handover scheduling, path diversity activation and Service Level Agreement (SLA) risk management.

II. RELATED WORKS

Recent work on radio-link failure prediction has focused on fusing temporal radio KPIs with meteorological forecasts and applying deep sequence models to flag impending outages. Islam et al. develop an LSTM–autoencoder trained on failure-free links that raises alarms via reconstruction error and combines spatial merging, one-hot encoding, PCA, SMOTE rebalancing and time-series cross-validation to predict next-day failures [1]. A broad survey formalizes lead-time and target-window concepts, catalogs supervised and unsupervised Network Fault Prediction (NFP) methods (tree ensembles, SVMs, AEs/LSTMs, GANs) and proposes a maintenance-aware cost metric that ties classifier outputs to SLA/logistics impact, providing evaluation criteria beyond conventional ROC/AUPR [2]. Kazi Hasan et al. in [3] replace heuristic weather-station selection with a differentiable, learnable GNN aggregator coupled to a time-series

transformer (GenTrap), improving precision/recall over LSTM baselines by endowing the model with weighted spatial context. Simba (an anomaly detection and root-cause analysis scheme for 5G RANs introduced by Antor Hasan et al. in [4]) fuses graph learning, graph convolutions and transformers to jointly detect and localize simultaneous, correlated base-station anomalies on calibrated Simu5G traces, demonstrating that explicit graph priors improve multi-site failure detection versus ConvLSTM/GNN baselines. Work from adjacent security domains shows how contrastive generative encoders plus metric learning can handle class imbalance and representation drift. For example, a contrastive variational autoencoder with deep metric learning for BCoT intrusion detection both learns discriminative embeddings and generates balanced synthetic attacks, highlighting techniques transferable to rare, weather-driven RLFs [5].

Representation learning via contrastive and predictive encoders has produced robust, transferable features across signal and temporal domains. Ren et al. in [6] propose ProbAuto-Aug and cross-view prediction in CPAA to learn OFDM modulation embeddings that hold up under extreme label scarcity and augmentation uncertainty. Sheng et al. present a Contrastive Predictive Autoencoder (CPR) in [7] that pairs autoregressive contrastive prediction with reconstruction on dynamic point clouds, learning multi-granularity spatio-temporal features that transfer well to downstream tasks. Xue et al. introduce MRSCD, a contrastive autoencoder for multivariate time series that constructs positive/negative pairs via multi-resolution randomized down-sampling and segment-consistency discrimination to reduce false negatives and improve anomaly F1 [8]. Several practical hybrids demonstrate the value of combining reconstruction and contrastive objectives: Dawei Luo et al. show that contrastive backbones plus AE regularization improve unsupervised OOD detection by tightening in-distribution clusters while reconstruction preserves feature stability [9], Nikougoftar applies autoencoder training with an added contrastive loss in an IoT outlier detection setting and proposes statistically grounded thresholding for unsupervised deployment [10], Pokkuluri et al. augment autoencoders with cellular automata dynamics to expose evolving spatial–temporal patterns that improve anomaly ROC-AUC and F1 where local coupling matters [11]. Collectively, these works teach two relevant lessons for radio-weather modeling: (i) carefully designed augmentation and multi-view contrastive tasks reduce false negatives and improve shift robustness and (ii) pairing discriminative contrastive losses with reconstruction or generative modules stabilizes embeddings for downstream scoring or synthesis.

Survival and time-to-event methodology provides a principled way to convert scores into actionable "when" estimates, but it is underused in RLF literature. The Kaplan–Meier product-limit estimator remains the canonical nonparametric tool for censored lifetimes and staggered-entry designs; Pollock and the classical Kaplan–Meier exposition under-pin practical survival curve estimation and confidence bands used in many applied domains, especially in medical research [12-15]. Recent deep survival work shows how multimodal feature extractors and mixture-of-Cox or deep nonparametric regressors can yield calibrated time-to-event predictions: Zhao et al. integrate radiomics, ViT features and immune signals into a self-adapted DCM pipeline (SA-DCM) to predict tumor progression and demonstrate how grouped feature representations and mixture models improve calibration and C-index [16]. Cui et al. optimize an autoencoder (DSACC), latent clustering and a contrastive loss to exploit correlations between censored and uncensored samples; their contrastive design improves C-index and Integrated Brier Score (IBS) by letting censored instances borrow supervision from uncensored anchors within learned clusters [17].

Most prior works on RLF prediction have been limited to binary classification, indicating only whether a failure will occur. They do not provide information on when failures are likely to happen. Our methodology closes this gap by modeling the timing of failures and providing actionable survival estimates.

III. Methodology

This section details the methodology adopted in this study, beginning with the dataset description and preprocessing procedures. An overview of the proposed workflow is then outlined, followed by the integration of weather station features through feature aggregation. Subsequently, the operation of the contrastive autoencoder is described, highlighting its role in anomaly detection through reconstruction error. Finally, the incorporation of survival analysis into the workflow is discussed, establishing its relevance to the overall analytical framework.

*A. **Dataset Description***

The dataset utilized in this study was provided by Turkcell, a major telecommunication service provider in Turkey [18]. To ensure privacy and security, the actual geo-locations were not disclosed; instead, a pairwise distance matrix between radio towers and weather stations was supplied.

Radio Link Dataset: The radio link dataset contains 1,387 site entries with both spatial and temporal characteristics. Key performance indicators (KPIs) form the core of this dataset, comprising 21 features that capture link performance. Among them, date-time, polarization, frequency band, link length, modulation, error seconds, severely errored seconds, unavailable seconds, available time and background bit error (BBE) were identified as the most influential attributes in characterizing link quality. Sequential dependencies are evident in features such as date-time, errored seconds, unavailable seconds, available time and BBE, while polarization, link length, modulation, clutter class, and ground height primarily reflect spatial properties. KPI samples were aggregated at a daily resolution for each radio link.

Weather Dataset: The real weather dataset was obtained from 112 stations for the same period and includes 16 attributes, of which temperature (maximum, minimum, current), wind direction (maximum, minimum), wind speed (maximum, minimum), humidity, precipitation, pressure, and sea-level pressure were identified as most impactful. Similar to the KPI dataset, several weather attributes exhibit sequential properties, while clutter class and ground height capture spatial characteristics of the stations.

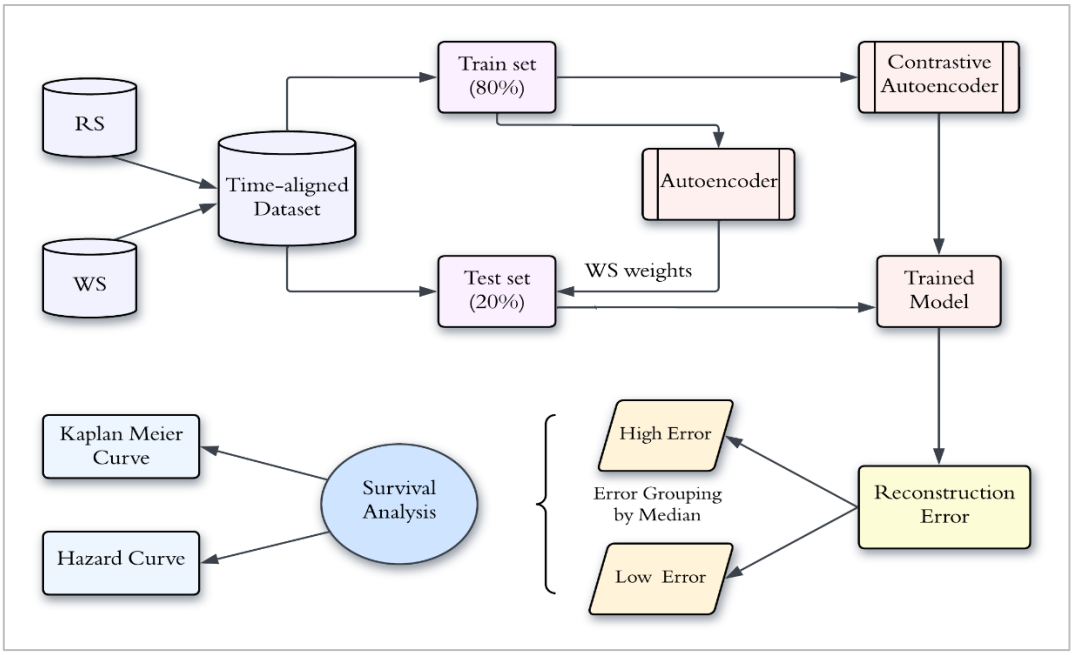

Figure 1. Proposed Model Architecture

The dataset spans a 12-month period (02-01-2019 to 31-12-2019). For this study, only the first four months were considered to maintain computational feasibility and reduce model training complexity. This subset contains a total of 250,339 data points, with the target variable defined as radio link failure (RLF). Among these, only 807 samples correspond to RLF events, indicating a highly imbalanced distribution that introduces additional challenges for predictive modeling.

B. Data Preprocessing

The dataset underwent a structured preprocessing procedure to address missing and inconsistent values. Missing entries in meteorological variables such as minimum and maximum temperature, humidity and wind speed were imputed using a localized mean approach, where each missing value was estimated from neighboring observations within the same link and temporal window. This preserves local temporal patterns while reducing bias from global averaging. Link length, being a static attribute per connection, was filled using the per-link average to ensure consistency. For the scalability score, missing values were replaced using localized medians, providing robustness against outliers. Categorical variables were imputed with the most frequent value within each link, maintaining coherence in link-level characteristics. Finally, all imputed values were subjected to physical plausibility checks, with temperature, humidity, wind speed and link length constrained within realistic ranges to avoid spurious imputations. This preprocessing ensured both statistical reliability and physical consistency of the dataset for subsequent analysis.

C. Proposed Architecture

In this study, the radio station (RS) dataset was first temporally aligned with the datasets of the three nearest weather stations (WS) to construct a unified dataset. This dataset was then partitioned into an 80%–20% split for training and testing respectively. The training set was initially processed using an autoencoder with a custom-defined loss function to estimate the relative contribution (weights) of the three WS features, which were subsequently applied to the test set.

Next, a contrastive autoencoder trained with a triplet loss function was employed on the training data to obtain a robust encoder representation. The trained encoder was applied to the test data to compute reconstruction errors, which were stratified into high-error and low-error groups using the median threshold. Survival analysis was then conducted on these groups. Figure 1 shows the complete proposed architecture and the detailed design and functionality of each methodological component are elaborated in the subsequent subsections.

D. Aggregation of WS Features

To capture the influence of local weather conditions on radio link failures (RLF) more comprehensively, each radio site (RS) was associated with multiple weather stations (WS) rather than a single source. Specifically, the three nearest WS were selected for each RS to ensure that spatial variations in meteorological conditions were adequately represented.

The association between RS and WS was established using a distance matrix provided by the service operator, specifying pairwise distances (in kilometers) between each RS site and every WS station. Since geographical coordinates were withheld for privacy, the distance matrix served as the only basis for linking RS to WS. For each RS, the three closest WS were identified and their features aggregated as triplets for meteorological parameters such as temperature, humidity, pressure, wind and precipitation.

A temporal misalignment existed between the datasets: RS records were available once per day at midnight, while WS records were logged hourly. To resolve this, WS features were time-aligned with RS entries using interpolation, ensuring that for every RS daily entry, corresponding WS triplet features were consistently matched.

In preprocessing, RS features were categorized into numerical attributes (e.g., link length, error seconds,

unavailable seconds, background bit errors, received level) and categorical attributes (e.g., polarization, frequency band, modulation, adaptive modulation). Numerical features were median-imputed and standardized, while categorical features were mode-imputed and one-hot encoded. Similarly, WS triplet features were interpolated, mean-imputed and standardized to mitigate inter-station variability.

The final input representation thus consisted of site-specific RS features enriched with temporally aligned and spatially aggregated WS triplets, providing a unified dataset for subsequent learning models. An autoencoder was then employed to assign relative weights to the three nearest WS features and compress them into a single representative feature vector, capturing the most informative aspects of local weather conditions for each RS site.

E. Supervised Autoencoder for WS Feature Fusion

An autoencoder is a type of neural network designed to learn a compressed representation (encoding) of input data by minimizing the difference between the input and its reconstruction. In anomaly detection, the reconstruction error serves as a measure of deviation from normal patterns, allowing the identification of outlier instances. Figure 2 shows the architecture of a vanilla encoder.

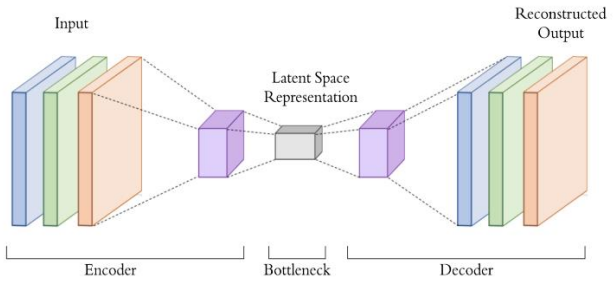

Figure 2. Autoencoder Architecture

Technical Architecture of the Proposed Autoencoder:
From the training dataset, each weather station feature set is processed independently using a deep symmetric dense autoencoder with the following structure:

- **Encoder path:**
  - Input: 3 neurons (one per weather station in the group).
  - Dense layer: 8 neurons, ReLU activation.
  - Dense layer: 4 neurons, ReLU activation.
  - Bottleneck (latent): 1 neuron (linear + LeakyReLU activation).
- **Decoder path:**
  - Dense layer: 4 neurons, ReLU.
  - Dense layer: 8 neurons, ReLU.
  - Output: 3 neurons (linear activation, to reconstruct original weather station inputs).

Thus, each group of 3 correlated weather features is reduced to a single latent variable. All latent variables across groups are concatenated into a fused weather vector. The use of Leaky ReLU in the bottleneck prevents dead neurons and enables the latent node to capture both positive and negative variations, ensuring that important negative correlations (e.g., pressure drops) are not suppressed.

Supervised RLF Prediction Head:
The concatenated fused weather vector is further supervised by an additional prediction pathway:

- Fused weather vector → Dense (16, ReLU) → Dense (1, Sigmoid)

This structure enforces that the fused latent weather representation is not only useful for reconstruction, but also predictive of RLF. The 16-neuron dense layer serves as a non-linear transformation layer that learns higher-order interactions across weather features before compressing into a final 1-neuron sigmoid output, which predicts RLF probability. Figure 3 shows the entire supervised autoencoder framework.

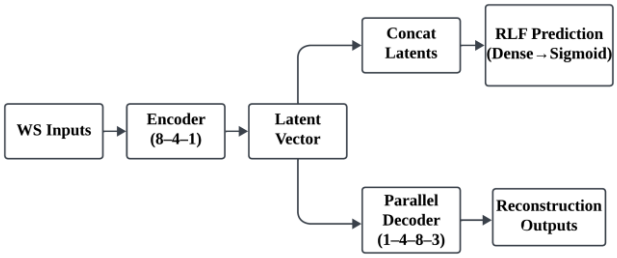

Figure 3. Supervised Autoencoder Framework

Loss Function Formulation:
A key innovation in this autoencoder is the incorporation of supervised predictive loss alongside reconstruction loss. Let X_{WS} represent the WS triplet input, X'_{WS} the reconstructed triplet and $\hat{Y}_{RL}$ the predicted radio link failure (RLF) probability. The total loss L_{total} is defined as:

$$L_{total} = \alpha \cdot MSE(X_{WS}, X'_{WS}) + \beta \cdot BCE(Y_{RL}, \hat{Y}_{RL}) \quad (1)$$

where, α=0.5 and β=1, MSE = Mean Square Error, BCE = Binary Cross Entropy, reflecting the priority of predictive supervision over reconstruction. This design ensures that the fused WS feature vector captures patterns relevant to RLF prediction, rather than solely reconstructing input values, thereby enhancing the interpretability and utility of the latent representation.

All the aforementioned processing and training were performed on the training dataset and the learned autoencoder weights for each WS feature group were applied to the test set, transforming its WS triplets into latent representations and forming fused weather vectors for RLF prediction.

F. Contrastive Autoencoder for Reconstruction-Based RLF Analysis

To capture complex relationships among weather and radio link features while emphasizing the distinction between normal and failure conditions, a contrastive autoencoder (CAE) was employed. Unlike standard autoencoders, the CAE integrates contrastive learning via triplet loss, which encourages the latent representations of normal samples to cluster together while separating failure samples in the latent space. This property enhances the autoencoder's ability to detect deviations from typical patterns through reconstruction error.

Network Architecture:
The CAE is a fully connected dense autoencoder with symmetric encoder-decoder architecture, designed to map

input features $X \in \mathbb{R}^d$, where d is the number of output neuron, into a compact latent space and reconstruct the original inputs. The encoder progressively reduces dimensionality, while the decoder mirrors this structure to reconstruct the input. The detailed layer-wise functionality is shown in Table 1.

Table 1: Layer-wise functionality of CAE

Layer	Activation	Function
Encoder 1	ReLU	Initial feature extraction
Encoder 2	ReLU	Intermediate abstraction
Encoder 3	ReLU	Latent compression
Encoder 4/Bottleneck	ReLU	Compact latent representation
Decoder 1	ReLU	Upsampling latent features
Decoder 2	ReLU	Further reconstruction
Decoder 3	ReLU	Reconstruction expansion
Output	Linear	Reconstruct original features

Figure 4 outlines the proposed CAE architecture.

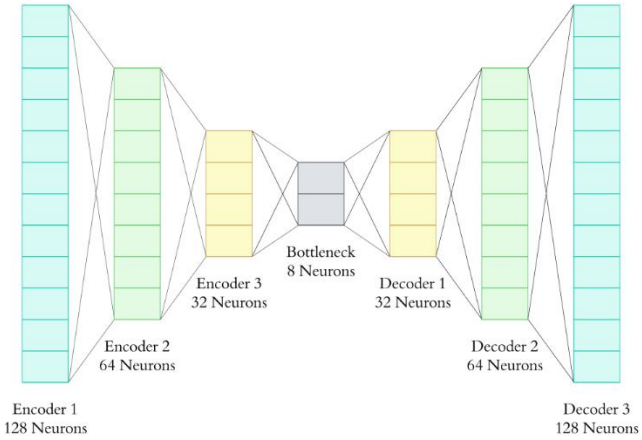

Figure 4. Proposed CAE architecture

The encoder outputs serve as the latent representation of each sample, which is further manipulated through triplet contrastive learning.

Triplet Loss and Latent Space Manipulation

In this work, triplets are constructed from the training set as follows:

- Anchor (a): a normal sample.
- Positive (p): another normal sample.
- Negative (n): a failure sample.

These triplets are used to train the autoencoder in a self-supervised manner, encouraging the latent representation of the anchor to be closer to the positive and farther from the negative in latent space. The triplet loss function is defined as:

$$L_{triplet} = \frac{1}{N}\sum_{i=1}^{N} max\,(pos\_dist_i - neg_{dist_i} + margin, 0) \quad (2)$$

where, $pos\_dist_i = \frac{1}{d}\sum_{j=1}^{d}(a_{ij} - p_{ij})^2$;

$$neg\_dist_i = \frac{1}{d}\sum_{j=1}^{d}(a_{ij} - n_{ij})^2$$

and margin is a hyperparameter enforcing a minimum separation between anchor-positive and anchor-negative pairs. Here, d is the input dimension and N is the number of triplets.

Through this mechanism, the latent space is structured such that normal radio conditions cluster together, while RLF-inducing samples are pushed apart, ensuring that deviations from typical patterns are amplified.

In our case, the training dataset is fed into the CAE to learn the normal and failure representations and the trained model is then applied to the test dataset. Consequently, when a new test sample is reconstructed, the reconstruction error—calculated as the mean absolute deviation between the input and reconstructed vector—effectively captures anomalous behavior, thereby enabling survival analysis of RLF events. Table 2 shows the training parameter settings.

Table 2: Training Parameter Settings

Parameter	Value
Number of triplets generated for contrastive training	20,000
Mini-batch size for training	128
Number of training epochs	50
Margin	1

In this CAE framework, reconstruction error computed on test samples is used to stratify the dataset into high-error and low-error groups based on the median, enabling survival analysis that correlates latent-space anomalies with radio link failures.

G. Survival Analysis Framework

Survival analysis provides a statistical framework to model the time until the occurrence of an event of interest, making it particularly suitable for reliability studies and failure prediction. In the context of this work, survival analysis offers a novel dimension by linking weather-influenced reconstruction error patterns from the autoencoder to the temporal dynamics of RLF. This approach extends conventional classification-based prediction by explicitly incorporating the time-to-failure component, thereby enabling a deeper understanding of whether certain feature-driven error profiles accelerate the risk of network degradation.

For this purpose, the dataset was reformulated into a survival format, where each record contains a time variable representing the observation period and an event indicator denoting whether a failure occurred within that interval. This procedure is done to each of the RS. The reconstruction error obtained from the autoencoder was aggregated and used as a covariate to stratify samples into two groups: high-error and low-error. This grouping allows the error measure to serve as a surrogate for latent vulnerability, linking autoencoder-driven feature fusion with temporal reliability assessment.

The objective is to investigate whether the high-error group exhibits a significantly elevated hazard of failure compared to the low-error group over time. By structuring the analysis in this manner, survival modeling enables the quantification of how strongly reconstruction errors correlate with accelerated RLF risk, offering both predictive and interpretive value. This dual perspective not only validates the robustness of the error metric but also provides operators

with an evidence-based framework for preemptive network maintenance.

Kaplan-Meier Curve

Kaplan–Meier survival curves were employed to estimate the probability of radio link survival over time for the low and high error groups. The Kaplan–Meier estimator provides a non-parametric estimate of the survival function, explicitly accounting for censored observations where failures have not yet occurred. In this framework, stratifying samples based on reconstruction error allows for a direct comparison of time-to-failure distributions, highlighting whether higher reconstruction errors are associated with accelerated failure risk. Kaplan–Meier curves thus serve as a tool to quantify and visualize the temporal effect of error-driven vulnerability on network reliability, enabling statistical assessment of differences between groups.

Hazard Curve

Cumulative hazard curves were constructed using the Nelson–Aalen estimator to capture the instantaneous risk of failure over time. The hazard function quantifies the accumulation of failure intensity, providing a complementary perspective to the survival probability. High-error groups are expected to exhibit steeper hazard trajectories, reflecting elevated and accelerating risk, while low-error groups show more gradual hazard accumulation. By analyzing both Kaplan–Meier and hazard curves, the methodology links reconstruction-error measures to temporal reliability patterns, offering interpretable insights for preemptive network maintenance and risk assessment.

IV. Evaluation and Results

A. Original RLF Instances

The evaluation was conducted by first stratifying the dataset into low and high reconstruction error groups using the median reconstruction error as the threshold. All records with missing values in the time-to-event or event indicator fields were removed to ensure robust survival modeling. Kaplan–Meier survival curves and Nelson–Aalen cumulative hazard curves were then fitted separately for each group, using the original RLF instances from the test dataset to plot survival probability versus time-to-event. This setup enables direct observation of how reconstruction-error-driven stratification correlates with network failure dynamics over time.

The Kaplan–Meier survival curve (Figure 5) demonstrates that the low-error group maintains a relatively stable survival probability, with a shallow slope indicating slow degradation and a low likelihood of failure over the observed period. In contrast, the high-error group exhibits a steeper decline in survival probability, reflecting a higher and accelerating risk of failure.

Complementing this, the cumulative hazard curve (Figure 6) shows that the high-error group accumulates failure risk more rapidly, whereas the low-error group follows a gradual hazard accumulation, consistent with more stable network performance. Together, these curves illustrate that elevated reconstruction errors serve as a strong indicator of increased time-dependent failure risk, validating the utility of reconstruction-error-based stratification in assessing network reliability.

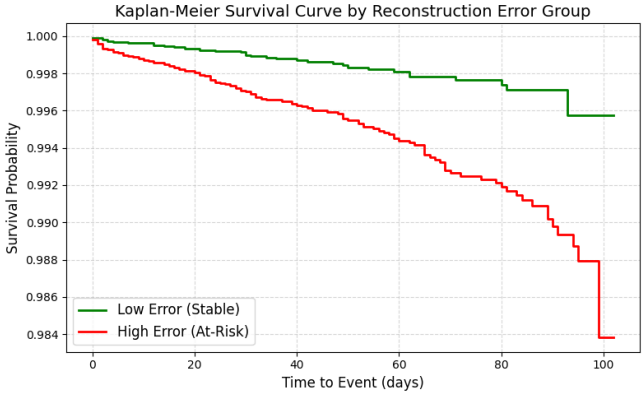

Figure 5. Kaplan–Meier Curve for original RLF instances

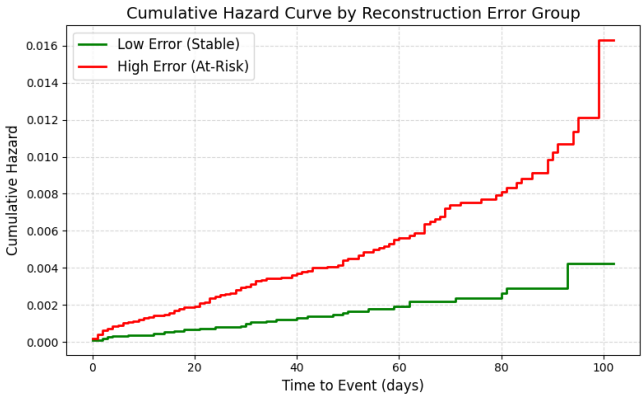

Figure 6. Hazard Curve for original RLF instances

B. Predictive Modeling

In the second evaluation stage, predictive modeling was employed to forecast RLF events based on reconstruction error patterns. The reconstruction errors obtained from the autoencoder were first used to train an *Isolation Forest* model. The model was fitted using non-failure reconstruction errors from the training set, enabling it to learn the normal behavior distribution. During testing, reconstruction errors were reshaped and input into the trained Isolation Forest, which classified instances as anomalies if the error exceeded the learned threshold. Formally, predicted anomalies were labeled as potential RLF events, providing a basis for predictive survival analysis. This method allows translation of unsupervised reconstruction error patterns into actionable RLF predictions.

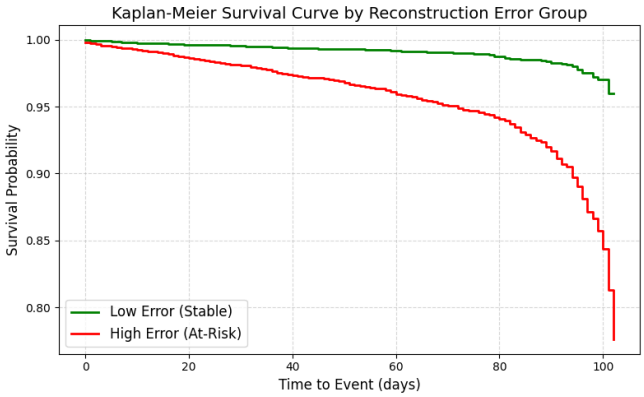

Figure 7. Kaplan–Meier Curve for predicted RLF instances

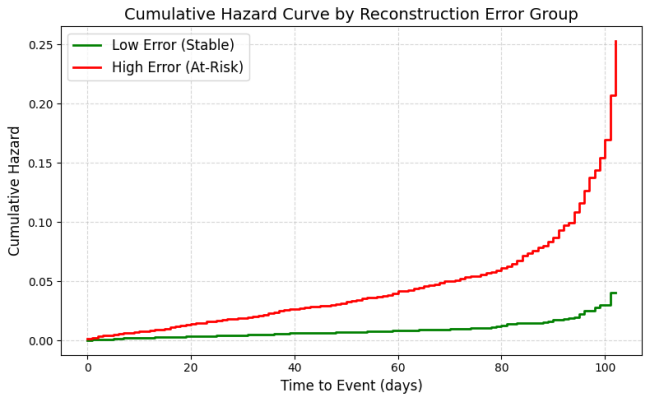

Figure 8. Hazard Curve for predicted RLF instances

For evaluation, Kaplan-Meier and cumulative hazard curves were plotted using RLF instances predicted by the Isolation Forest. High and low error groups were defined by median reconstruction error similar to the first section.

Kaplan–Meier curve (Figure 7) indicates that the high-error group has a higher risk of RLF over time, while Nelson–Aalen curve (Figure 8) shows faster hazard accumulation for this group. This predictive analysis complements the original RLF-based evaluation, demonstrating the effectiveness of reconstruction-error-driven anomaly detection for forecasting network failures.

V. CONCLUSION

This study proposed a weather-aware RLF prediction framework that jointly addresses failure detection and time-to-event estimation under dynamic meteorological variations. Leveraging a supervised autoencoder for triplet-based weather feature fusion, a contrastive autoencoder (CAE) with triplet loss for learning discriminative latent embeddings and non-parametric survival analysis for temporal reliability modeling, the framework achieves calibrated, per-link time-to-failure predictions. Experimental results demonstrate that reconstruction-error-driven stratification strongly correlates with elevated hazard rates, validating the effectiveness of latent anomaly patterns in predicting RLF dynamics. The novelty of this work lies in the integration of contrastive representation learning with survival modeling, enabling interpretable, actionable and weather-sensitive reliability insights that extend beyond conventional binary RLF classifiers.

For future work, we aim to extend this framework by incorporating advanced deep survival models such as DeepSurv, DeepHit and Cox-Time architectures, enabling joint modeling of censored time-to-failure distributions while leveraging multimodal features. Such extensions will further enhance calibration, generalization and operational applicability in next-generation weather-sensitive wireless networks.

REFERENCES

[1] M. A. Islam, H. Siddique, W. Zhang and I. Haque, "A Deep Neural Network-Based Communication Failure Prediction Scheme in 5G RAN," *IEEE Trans. Netw. Serv. Manag.*, vol. 20, no. 2, pp. 1140–1152, Jun. 2023, doi: https://doi.org/10.1109/TNSM.2022.3229658.

[2] K. Murphy, A. Lavignotte and C. Lepers, "Fault Prediction for Heterogeneous Telecommunication Networks Using Machine Learning: A Survey," *IEEE Trans. Netw. Serv. Manag.*, vol. 21, no. 2, pp. 2515–2538, Apr. 2024, doi: https://doi.org/10.1109/TNSM.2023.3340351.

[3] K. Hasan, K. Papry, T. Trappenberg and I. Haque, "A Generalized GNN-Transformer-Based Radio Link Failure Prediction Framework in 5G RAN," *IEEE Trans. Mach. Learn. Commun. Netw.*, vol. 3, pp. 710–724, 2025, doi: https://doi.org/10.1109/TMLCN.2025.3575368.

[4] A. Hasan, C. Boeira, K. Papry, Y. Ju, Z. Zhu and I. Haque, "Root Cause Analysis of Anomalies in 5G RAN Using Graph Neural Network and Transformer," *arXiv preprint arXiv:2406.15638*, Jun. 2024, doi: https://doi.org/10.48550/arXiv.2406.15638.

[5] C. Wu, X. Liu, K. Ding *et al.*, "Attack Detection Model for BCoT Based on Contrastive Variational Autoencoder and Metric Learning," *J. Cloud Comput.*, vol. 13, no. 125, 2024, doi: https://doi.org/10.1186/s13677-024-00678-w.

[6] B. Ren, Z. Su, K. C. Teh, H. An, E. Gunawan and A. C. Kot, "CPAA: Self-Supervised Cross-View Prediction with Automatic Augmentation for OFDM Modulation Classification," *IEEE Trans. Veh. Technol.*, vol. 74, no. 7, pp. 10536–10550, Jul. 2025, doi: https://doi.org/10.1109/TVT.2025.3543800.

[7] X. Sheng, Z. Shen and G. Xiao, "Contrastive Predictive Autoencoders for Dynamic Point Cloud Self-Supervised Learning," in *Proc. AAAI Conf. Artif. Intell.*, vol. 37, no. 8, pp. 9802–9810, 2023, doi: https://doi.org/10.1609/aaai.v37i8.26170.

[8] B. Xue, X. Gao, F. Zhai *et al.*, "A Contrastive Autoencoder with Multi-Resolution Segment-Consistency Discrimination for Multivariate Time Series Anomaly Detection," *Appl. Intell.*, vol. 53, pp. 28655–28674, 2023, doi: https://doi.org/10.1007/s10489-023-04985-8.

[9] D. Luo, H. Zhou, J. Bae and B. Yun, "Combining Contrastive Learning with Auto-Encoder for Out-of-Distribution Detection," *Appl. Sci.*, vol. 13, no. 23, p. 12930, 2023, doi: https://doi.org/10.3390/app132312930.

[10] E. Nikougoftar, "Outlier Detection in IoT Using Trained Autoencoder and Contrastive Loss," *preprint*, Research Square, Aug. 19, 2024, doi: https://doi.org/10.21203/rs.3.rs-4657376/v1.

[11] P. K. Sree *et al.*, "Auto Encoders with Cellular Automata for Anomaly Detection," in *Cognitive Computing and Cyber Physical Systems (IC4S 2024)*, vol. 598, Cham: Springer, 2025. doi: https://doi.org/10.1007/978-3-031-77078-4_28.

[12] M. Deng, Q. Li, Z. Zhang *et al.*, "Survival Analysis of PLWH on Antiretroviral Therapy in Henan Province From 2004 to 2024," *Sci. Rep.*, vol. 15, p. 21322, 2025, doi: https://doi.org/10.1038/s41598-025-05821-4.

[13] A. Chaddad, L. Hassan, Y. Katib and A. Bouridane, "Deep Survival Analysis with Clinical Variables for COVID-19," *IEEE J. Transl. Eng. Health Med.*, vol. 11, pp. 223–231, 2023, doi: https://doi.org/10.1109/JTEHM.2023.3256966.

[14] K. Duman, J. Powell, S. Thomas and E. Spezi, "Evaluation of Radiomic Analysis Over the Comparison of Machine Learning Approach and Radiomic Risk Score on Glioblastoma," in *Proc. Cardiff University Engineering Research Conference 2023*, pp. 19–22, 2024, doi: http://dx.doi.org/10.18573/conf1.f.

[15] K. H. Pollock, S. R. Winterstein, C. M. Bunck and P. D. Curtis, "Survival Analysis in Telemetry Studies: The Staggered Entry Design," *J. Wildl. Manage.*, vol. 53, no. 1, pp. 7–15, Jan. 1989 [Online]. Available: https://www.jstor.org/stable/3801398.

[16] Z. Zhao, W. Li, P. Liu, A. Zhang, J. Sun and L. X. Xu, "Survival Analysis for Multimode Ablation Using Self-Adapted Deep Learning Network Based on Multisource Features," *IEEE J. Biomed. Health Inform.*, vol. 28, no. 1, pp. 19–30, Jan. 2024, doi: https://doi.org/10.1109/JBHI.2023.3260776.

[17] C. Cui, Y. Tang and W. Zhang, "Deep Survival Analysis with Latent Clustering and Contrastive Learning," *IEEE J. Biomed. Health Inform.*, vol. 28, no. 5, pp. 3090–3101, May 2024, doi: https://doi.org/10.1109/JBHI.2024.3362850.

[18] M. A. Islam, "The data and code repository." 2022. [Online]. Available:https://github.com/ArifulIslamPreence/-RLFPredictionMainThesis